Макрогетероциклы
http://macroheterocycles.isuct.ru

DOI: 10.6060/mhc181224z

Excited States Relaxation in Covalently Linked Dyads and Triads Based on Tryptophan, Deuteroporphyrin and Naphthoquinone

Eduard I. Zenkevich,[a@] Ekaterina A. Larkina,[b] Nadezhda V. Konovalova,[b] and Alexander P. Stupak[c]

[a]*National Technical University of Belarus, 220013 Minsk, Belarus*
[b]*MIREA – Russian Technological University, M.V. Lomonosov Institute of Fine Chemical Technologies, 119571 Moscow, Russia*
[c]*B.I. Stepanov Institute of Physics NAS B, 220072 Minsk, Belarus*
[@]*Corresponding author E-mail: zenkev@tut.by*

Steady-state and time-resolved spectral-fluorescent characteristics have been measured for covalently linked dyads and triads consisting of deuteroporphyrin IX being attached via β-positions either to naphthoquinone or to one or two tryptophan residues in solutions of various polarity at 293 K. For the tryptophan-porphyrin dyad it was shown that experimental (Φ_{ET}^{exper}=0.75) and theoretical (Φ_{ET}^{theor}=0.87) values of the energy transfer efficiency are in a reasonable agreement and the Foerster theory of inductive resonance is still applicable to weakly interacting donor-acceptor systems at intercenter distances R_{DA}≈19÷25 Å. For the porphyrin-quinone dyad and tryptophan-porphyrin-quinone triad in dimethylformamide at 293 K, it was argued that the porphyrin fluorescence quenching may be appropriately described by the semi-classical Marcus theory as an endergonic or moderately exergonic non-adiabatic photoinduced electron transfer occurring within the "normal" region with the rate constant k_{PET}=2.7·10^8 s^{-1}. The quantitative experimental and theoretical analysis of both energy and photoinduced electron transfer processes for the systems under study leads to the conclusion that the formation of folded conformations is hardly realized for the dyads and triads in liquid solvents at ambient temperature.

Keywords: Deuteroporphyrin, tryptophan, quinone, covalently linked dyads and triads, non-radiative deactivation of singlet excited states, Foerster resonance energy transfer, photoinduced electron transfer.

Релаксация возбужденных состояний в ковалентно связанных диадах и триадах на основе триптофана, дейтеропорфирина и хинона

Э. И. Зенькевич,[a@] Е. А. Ларкина,[b] Н. В. Коновалова,[b] А. П. Ступак[c]

[a]*Белорусский национальный технический университет, 220013 Минск, Беларусь*
[b]*МИРЭА – Российский технологический университет, Институт тонких химических технологий им. М.В. Ломоносова, 119571 Москва, Россия*
[c]*Институт физики им. Б.И. Степанова НАН Б, 220072 Минск, Беларусь*
[@]*E-mail: zenkev@tut.by*

Для диад и триад, состоящих из дейтеропорфирина IX и хинона или одной либо двух молекул триптофана, ковалентно присоединенных по остаткам пропионовой кислоты в β-положениях порфирина, выполнены измерения стационарных и время-разрешенных спектрально-флуоресцентных характеристик в растворах различной полярности при 295 К. Для диад триптофан-порфирин было показано, что экспериментальные ($\Phi_{ПЭ}^{эксперт}$=0.75) и теоретические ($\Phi_{ПЭ}^{теор}$=0.87) значения эффективности переноса энергии находятся в разумном соответствии, и теория индуктивного резонанса Ферстера применима для слабо взаимодействующих донорно-акцепторных систем на расстояниях $R_{ДА}$≈19÷25 Å. Для диады порфирин-хинон и триады триптофан-порфирин-хинон в диметилформамиде при 293 К обосновано, что тушение флуоресценции порфирина может

быть адекватно описано полуклассической теорией Маркуса как эндотермический или слабо экзотермический неадиабатический фотоиндуцированный перенос электрона, происходящий в «нормальной» области с вероятностью $k_{ФПЭ}=2.7\cdot10^{8}$ c^{-1}. На основании количественного экспериментального и теоретического анализа процессов переноса энергии и фотоиндуцированного переноса электрона обосновано, что формирование свернутых конформаций диад и триад маловероятно в жидких растворителях при комнатной температуре.

Ключевые слова: Дейтеропорфирин, триптофан, хинон, ковалентно связанные диады и триады, безызлучательная дезактивация синглетных возбужденных состояний, ферстеровский резонансный перенос энергии, фотоиндуцированный перенос электрона.

Introduction

At the moment, on the basis of a combination of X-ray measurements together with steady-state, time-resolved and single molecule spectroscopy data it is well documented[1-6, and ref. herein] that photosynthesis is one of the finest piece of nanoscale molecular machinery where Nature utilizes the self-assembly principles to form multicomponent arrays of tetrapyrrole molecules and other organic substances for the directed fast and efficient energy transfer (ET) among light-harvesting pigment-protein antenna complexes to the photochemical reaction center where the energy of excited states is converted into a stable transmembrane charge separation through a sequence of photoinduced electron transfer (PET) reactions. In fact, the most complex and spectacular sets of tetrapyrrole containing self-organized arrays are found in photosynthetic objects. The elucidation of the mechanisms and dynamics of ET processes in light-harvesting antenna complexes as well as the intrinsic features of PET (such as charge separation and charge recombination of the product ion pair state) *in vivo*, are still the most fundamental and important problems. In fact, some aspects of the light collection and distant electron transfer reactions remain still non-understood yet in great detail from both experimental and theoretical background: i) the role of pigment-protein interactions and electronic couplings *via* bridge in the directed ET and PET processes, ii) electronic couplings and optimized energy transfer in confined molecular assemblies, iii) the relatively weak temperature dependence and high efficiency of charge separation, *etc*.

In this respect, the formation and study of artificial multiporphyrin/multichlorophyll assemblies and/or nanostructures containing tetrapyrrolic compounds and other functional organic/inorganic components are of fundamental importance as models for mimicking and the detailed study of ET and PET processes taking place within *in vivo* objects.[7-15, and ref. herein] The covalent linkage between supposedly essential components is considered to be one way of the supramolecular chemistry which provides a vast range of diverse supramolecular systems. Covalently linked multichromophoric systems possess favorable characteristics for light harvesting and/or charge separation.

On the other hand, the bottom-up construction of supramolecular nanodevices including organic and inorganic subunits offers a formidable challenge on the road towards modern nanotechnology.[16-20] This field is a new frontier of research that combines the building blocks of life and synthetic structures, both of them at a tiny, molecular-sized level. Its focus is on the development of powerful techniques and methods that merge the strengths of nanotechnology, working typically in the range of 1 to 100 nanometers, and biophysics, to generate a new type of 'bionanomaterial' which has some uniquely designed properties. In this respect, the interest in emerging nanostructures (including those based on tetrapyrrolic macrocycles) is growing exponentially since they are not only good models for the mimicking the primary photoevents *in vivo* but seems to be considered as promising building blocks for advanced multifunctional nanocomposites with potential applications in various fields of material science and nanobiomedicine.[21,22]

With these ideas in mind, on the first step we have prepared covalently linked organic dyads on the basis of deuteroporphyrin attached *via* β-positions to naphthoquinone or to one or two tryptophane residues. The detailed analysis of the structure and energy relaxation processes in these complexes have been used on the next step upon study regularities and mechanisms of the non-radiative deactivation of excited singlet states for tryptophane and porphyrin subunits in covalently linked tryptophane–porphyrin–quinone triad complex. Presumably the quantitative study of the non-radiative energy transfer and photoinduced electron transfer processes was mainly carried out for the given dyads and triad with known composition and morphology. The choice of deuteroporphyrin IX for the formation of dyads and triad is caused by the fact that the existence of two carboxylic groups permits to covalently attach two other subunits possessing variable donor or acceptor properties with respect to energy/electron transfer. In addition, the existence of propionic acid residues in deuteroporphyrin IX molecule gives the possibility to form conformations of the multicomponent complexes in which the intercenter distances between interacting moieties seem to be enough for appropriate energetic interactions. Amino acid component, tryptophan, was used as a potential donor of the energy or electron. In addition, it is known that amino acid residues in reaction centers *in vivo* may stabilize the charge transfer state in the energy scale,[23,24] and the existence of the dipole moment in tryptophan molecule may promotes the effective charge transfer.[25,26] It is well documented also that the fast and effective transformation of the electronic excitation energy into the energy of charge separated states in reaction centers *in vivo* is realized with participation of quinone molecules.[27-29] Correspondingly, like in the most artificial multimolecular systems modelling the primary photosynthetic events[e.g. 30-37] we have used quinone molecule also.

Finally, we would like to mention that this contribution is dedicated to the 85th anniversary of the world-known

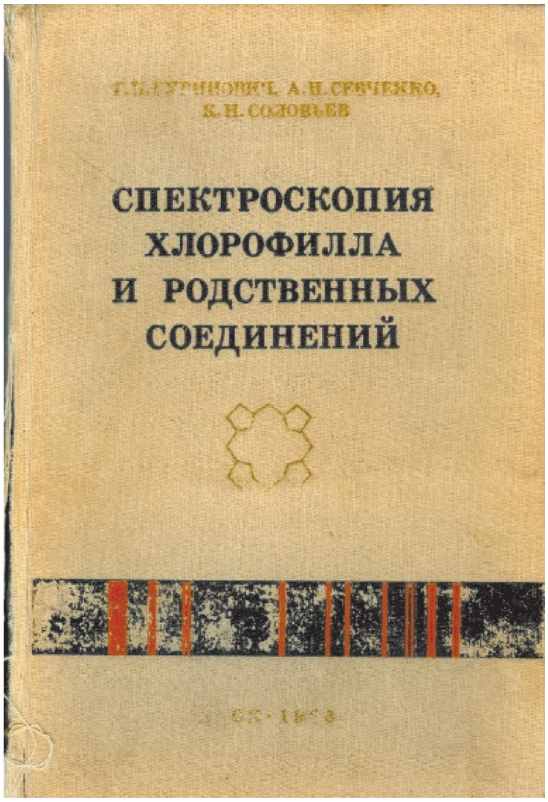

expert in photophysics and photochemistry of chlorophyll and related compounds academician G.P. Gurinovich (born in 1933), who was a real leader in this field, being an initiator and participant of a lot of pioneering and fruitful experimental investigations of spectral and energetic properties of tetrapyrrolic pigments in molecular state as well as in structurally organized complexes of various composition and morphology. Within few decades his book «Spectroscopy of Chlorophyll and Related Compounds»[38] was a real textbook for beginners, PhD students and other scientists working in this interesting and promising area of science.

Experimental

Materials

Covalently linked dyads and triads. Basic compound 2,7,12,18-tetramethyl-13,17-bis(2-methoxycarbonylethyl)porphine (deuteroporphyrin IX, **Dp**) has been obtained from haemin by method described earlier.[39] The synthesis of dyad containing naphthoquinone (Q) and deuteroporphyrin IX (1,3,5,8-tetramethyl-6(7)-{2-[2-(3-methyl-1,4-naphthoquinon-2-yl)thioethyl] oxycarbonylethyl}-7(6)-(2-carboxyethyl)porphyrin) has been carried using method described in.[40] The synthesis of tryptophan (Trp)-containing derivatives of deuteroporphyrin IX and triad containing molecules of Dp, Q and Trp has been carried using method described in.[41,42] The structures of dyads and triads have been supported by UV-VIS, IR and NMR spectroscopy and mass spectrometry.[40,42] Chemical structures of Dp, Trp and Q molecules as well covalently linked dyads and triads are presented in Figure 1.

For further analysis of experimental results on ET/PET rate constants the optimized geometries have been calculated for

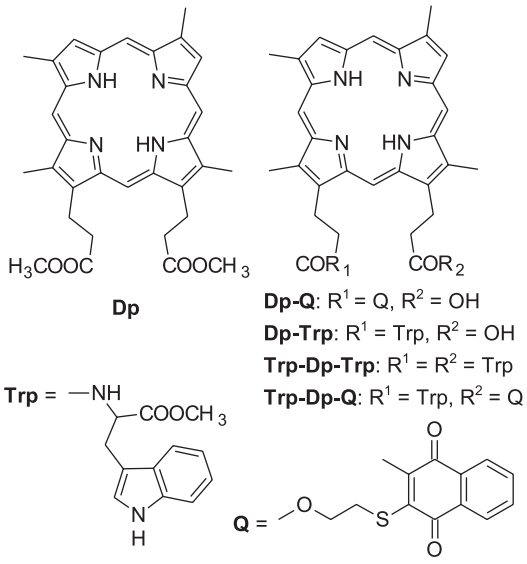

Figure 1. Chemical structures of dimethyl ester of deuteroporphyrin IX (Dp), tryptophan (Trp), quinone (Q) as well as dyads and triads under investigation.

some dyads and triad (Figure 2). It was found (using HyperChem 7.0 Pro, semiempirical methods AM1 or PM3) that two possible conformations may be realized: unfolded and folded (more optimized) (see Figure 2A and 2B, correspondingly). For the dyad **Dp-Q**, estimated intercenter distance is 19 Å (case A) and 4 Å (case B). Optimized geometry for triad **Trp-Dp-Q** has been calculated using Autodesk HyperChem (versions 2.0 and 3.0, MM^+ method) (Figure 2C, D). Because of flexibility of the covalent spacer the triad geometry is determined by the rotation of its fragments. At the beginning the calculation of the geometry with the minimal energy has been carried out by a sequential changing of pair of torsion angles (from 0 to 350°, 10° iteration, optimization by Newton-Rafson method with gradient 0.01 kcal/(Å·mol)). Final optimization has been done by Fleatcher-Rives method with gradient 0.01 kcal/(Å·mol). The whole energy of the optimized geometry for the triad **Trp-Dp-Q** was estimated to be 86.73 kcal/mol. In this case, the quinone subunit plane is practically parallel to the porphyrin plane with interplane distance of 3.23–3.96 Å, while the angle between the tryptophan and the porphyrin planes is ~ 45–50° with estimated distance 3.10–3.28 Å (Figure 2C). Calculations show also that from energetic point of view another geometry for the triad **Trp-Dp-Q** may be realized where both Q and Trp subunits are located together with respect to Dp macrocycle plane (Figure 2D).

Nevertheless, the flexibility of a covalent spacer may lead to the existence of few other conformations for the triad in which the indole ring may be moved away from the porphyrin subunit. Such fast transitions between conformations in liquid solutions at ambient temperature (compared to a time-scale of NMR measurements) manifest themselves in the broadening of proton peaks for tryptophan indole ring in NMR ^{1}H spectra and the absence of registered proton signals for $C_{\delta 1}$ and N atoms of tryptophan indole ring. However, the addition of 5 vol.% trifluoroacetic acid to solutions of compounds **Dp-Trp** and **Trp-Dp-Trp** in $CDCl_3$ or introduction of a Zn atom into the porphyrin macrocycle restrict the conformational mobility of the complexes which manifests itself in the appearance of two signals due to protons at the $C_{\delta 1}$ and N atoms in the ^{1}H NMR spectra. The detailed analysis of NMR data for the systems under study is presented in.[42] In addition, some structural properties of the dyad and triad were confirmed also on the basis of IR- and mass-spectrometry measurements.

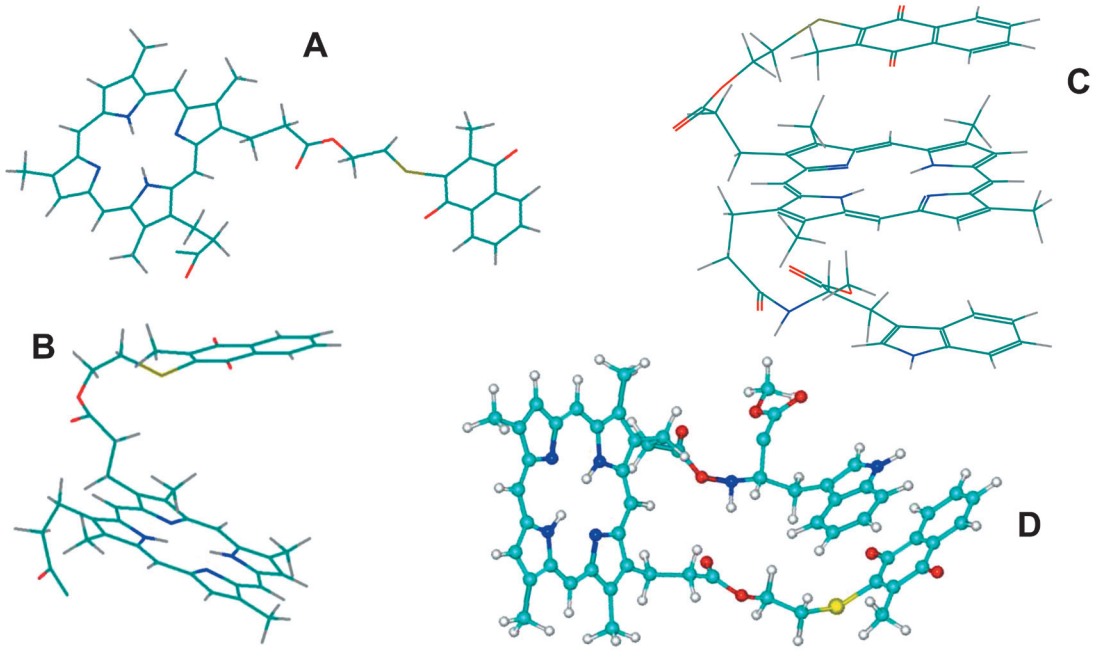

Figure 2. Optimized unfolded (A, D) and folded (B, C) geometries for the dyad **Dp-Q** (A, B) and for the triad **Trp-Dp-Q** (C, D).

Solvents

Solvents of various polarity (Aldrich, spectroscopic grade) such as methylcyclohexane, chloroform, toluene, tetrahydrofurane and dimethylformamide have been used at ambient temperature without further purification. Spectral steady-state and time-resolved measurements have been carried out in quartz optical cuvettes (Hellma QS 27 111, path length 1 cm). Optical density of solutions was OD≤0.15 in order to avoid reabsorption effects. Experiments have been completed during 1–2 h after sample preparation.

Spectral and Time-resolved Measurements

Absorption spectra were recorded with a Shimadzu 3001 UV/Vis or a Cary-500 M Varian spectrophotometer. Emission spectra were measured using spectrofluorophotometer SFL 1211A (Solar) as well as a home-built high-sensitive temperature variable laboratory set-up described earlier.[43] The fluorescence quantum yields φ_F of the systems under investigation were measured by the relative method,[44] tetraphenylporphyrin in non-degassed toluene (φ_F=0.09 at 293 K[45]) was used as a standard.

Time-resolved photoluminescence (PL) measurements on ensembles were performed in a time-correlated single photon counting mode under right-angle geometry using a laboratory pulse fluorometer PRA-3000 equipped with computer module TCC900 (Edinburg Instruments) and light emitting diodes PLS-8-2-130 (λ_{max}=457 nm, FWHM ~ 713 ps) or PLS-8-2-135 (λ_{max}=409 nm, FWHM ~ 990 ps; PicoQuant GmbH). In most cases, repetition rate was 2.5 MHz, average power range was ~30 mW, the duration of kinetic measurements in every experiment have been adjusted to 10000 counts at decay curve maximum. In some cases multi-exponential decay curves $A(t)$ were fitted by few components A_i according to $A(t)=\Sigma A_i \cdot \exp(-t/\tau_i)$. A commercial software program was used for decay analysis with the minimisation of chi-square values χ^2.

Scheme 1 shows the relative position of excited states in the energy scale as well as main deactivation processes in the systems under study.

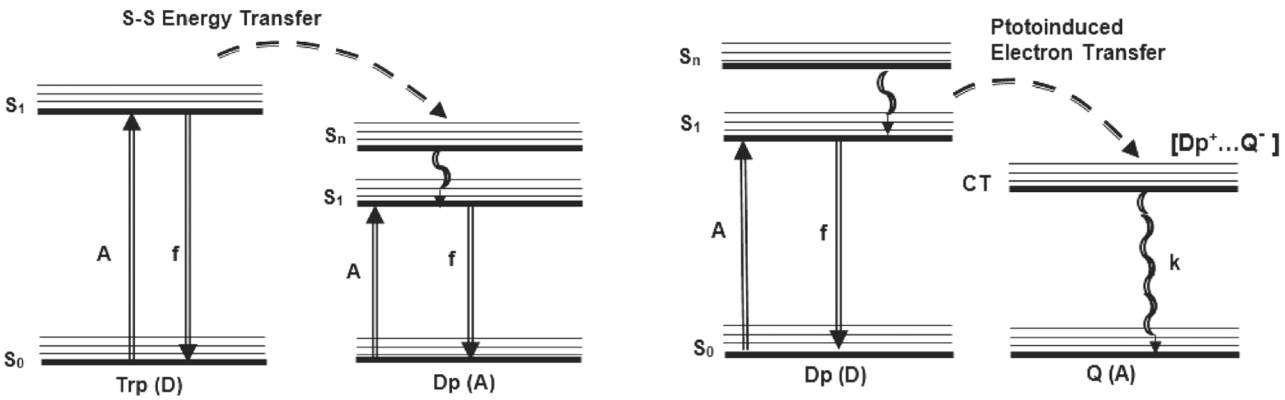

Scheme 1. Diagram of excited states and main relaxation processes in dyads **Trp-Dp** and **Dp-Q**. Rate constants of the main channels are as follows: absorption (A), fluorescence (f), non-radiative recombination of radical ion pair (k).

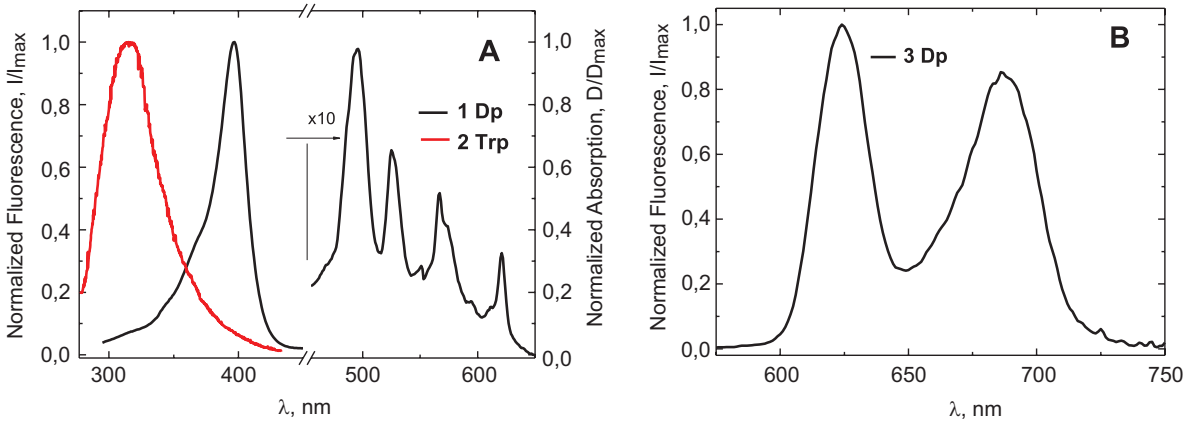

Figure 3. Absorption (1A) and fluorescence (2A, 3B) spectra of **Trp** (2) and **Dp** (1, 3) in toluene at ambient temperature (2A: λ_{exc}=240 nm; 3B: λ_{exc}=410 nm).

Results and Discussion

Spectral-kinetic Properties of Precursors, Dyads and Triads

It was found that absorption spectra of the triad **Trp-Dp-Trp** and dyad **Trp-Dp** are a linear combination of the corresponding spectra of monomeric precursors Trp and Dp without differences in wavelength maxima and band shapes (Figures. 3 and 4A). It means that the interaction between the two subunits is weak in the ground state, and they retain their individual identities.

At the same time, fluorescence spectra of the triad **Trp-Dp-Trp** and dyad **Trp-Dp** do show strong quenching of the Trp fluorescence (λ_{max}=330 nm) upon excitation at λ_{exc}=270 nm (Trp absorption band). In all cases the fluorescence spectra of the complexes mainly consist of Dp bands. Namely, in the dyad **Trp-Dp** the Trp fluorescence is absent practically (full quenching), while at low excitation level for the triad **Trp-Dp-Trp**, this band remains still visible but its intensity is quenched by >10 times with respect to that for the individual Trp at the same molar concentration. It is seen from Table 1 that the energetic interaction between Trp and Dp subunits in covalently linked complexes **Trp-Dp-Trp** and **Trp-Dp** manifesting in the strong quenching of Trp excited singlet state do not lead to the quenching of Dp excited singlet state (Table 1).

Data presented in Table 1 show that in toluene for alone Dp fluorescence lifetime τ_S is smaller than that measured in dimethylformamide. This difference is explained by two reasons. In toluene, the concentration of dissolved molecular oxygen [O_2] is higher and viscosity is smaller with respect to these values for dimethylformamide.[46] Thus, the quenching of Dp S_1 state by molecular oxygen is higher in toluene solutions compared to dimethylformamide. Our measurements have shown that in degassed solutions τ_S^0=18.1 ns for Dp. Based on these results one may conclude that fluorescence parameters of Dp in the triad **Trp-Dp-Trp** and dyad **Trp-Dp** do not change practically with respect to those for individual Dp molecules what is typical for acceptor molecules upon weak interaction with donor ones.[10,11,47-49] Energetic interactions between Trp and Dp in the dyad **Trp-Dp** manifest themselves in fluorescence spectra of the complex: upon excitation of the dyad at λ_{exc}=270 nm (Trp absorption band) Dp fluorescence intensity is stronger by 2 times compared to that for the individual Dp at the same molar concentration. Finally, it is seen from Figure 4B that fluorescence excitation spectra of the triad and dyad detected at Dp fluorescence band (λ_{det}≥640 nm) in tetrahydrofurane at 295 K clearly show the existence of absorption bands of Trp component in the region of 250–300 nm.

In the case of the triad **Trp-Dp-Trp** and dyad **Trp-Dp,** it seems reasonable to explain all the observed experimental findings as the manifestation of the inductive resonance energy transfer Trp→Dp with participation of excited singlet states of donor (D) and acceptor (A) molecules (S-S ET).[10,11,47-49] With respect to the given complexes,

Table 1. Fluorescence parameters for individual Dp, dyads and triad in solvents of various polarity at 295 K.

Solvent	Compound	Fluorescence quantum yield φ_F, %	Fluorescence decay τ, ns
Toluene	**Dp**	7.8	12.1
	Dp-Trp	8	12.3
	Dp-Q	3	9.3
	Trp-Dp-Q	5	8.7
Dimethylformamide	**Dp**	7.3	15.4
	Dp-Q	2	11.8 / 3.6
	Trp-Dp-Q	2.5	12.7 / 5.4

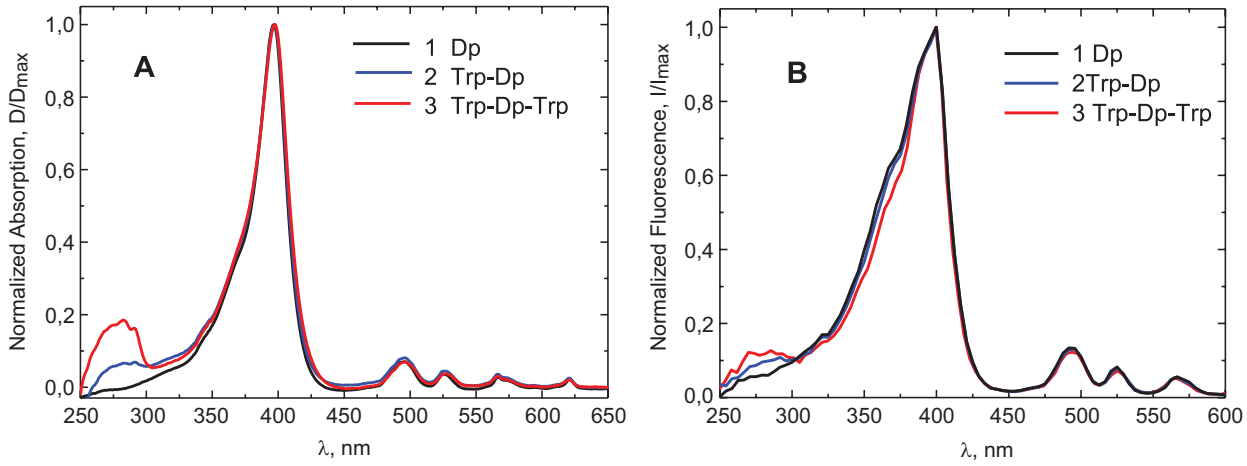

Figure 4. Absorption (A) and fluorescence excitation (λ_{det}=640 nm) (B) spectra of monomeric **Dp** (1), the dyad **Trp-Dp** (2) and the triad **Trp-Dp-Trp** (3) in tetrahydrofurane at 295 K.

the corresponding detailed analysis of these processes will be presented below.

Now let us consider properties of the dyad **Dp-Q** and triad **Trp-Dp-Q** containing electron accepting quinone subunit. Basic arguments showing that in these complexes the interaction between Dp and Q takes place with participation of the Dp excited singlet states are evident from fluorescence decay measurements and ps/ns pump-probe experiments (see Table 1 and Figure 5).

Compared to individual Dp molecules, in the dyad **Dp-Q** and triad **Trp-Dp-Q** the fluorescence of the porphyrin subunit is noticeably quenched manifesting in the decrease of the fluorescence quantum efficiency φ and decay τ shortening (Table 1, Figure 5A). In fact, these effects are typical for porphyrin-quinone systems of various morphology where the photoinduced electron transfer (PET) processes porphyrin→quinone are more or less effective depending on the system geometry, flexibility and D-A distances.[30-37] It is also seen from data presented in Table 1 that in toluene at ambient temperature, quenching effects are practically the same for both **Dp-Q** and **Trp-Dp-Q** complexes. On the other hand, in polar dimethylformamide Dp fluorescence quenching becomes more pronounced and, additionally, Dp emission decay becomes non-exponential. In addition, transient absorption spectra of **Dp-Q** show a noticeable spectral dynamics (Figure 5B). The rising absorption near 650–670 nm may be ascribed to Dp^+ species by referring to the corresponding spectra obtained by electrochemical oxidation of a porphyrin free base.[50,51] It should be mentioned also that relative quantum yields of Dp fluorescence in dyad (φ_{dyad}/φ_0) and triad ($\varphi_{triad}/\varphi_0$) with respect to that for individual Dp (φ_0) are weakly dependent on the solvent nature being slightly higher for triad in comparison with dyad: φ_{dyad}/φ_0=0.38, 0.4, 0.4, 0.28 and $\varphi_{triad}/\varphi_0$=0.64, 0.60, 0.55, 0.45 in toluene, chloroform, methylcyclohexane and dimethylformamide, correspondingly. This variation in relative quantum yields values may reflect different conformational mobility of subunits and steric interactions in the triad and dyad which may also be dependent

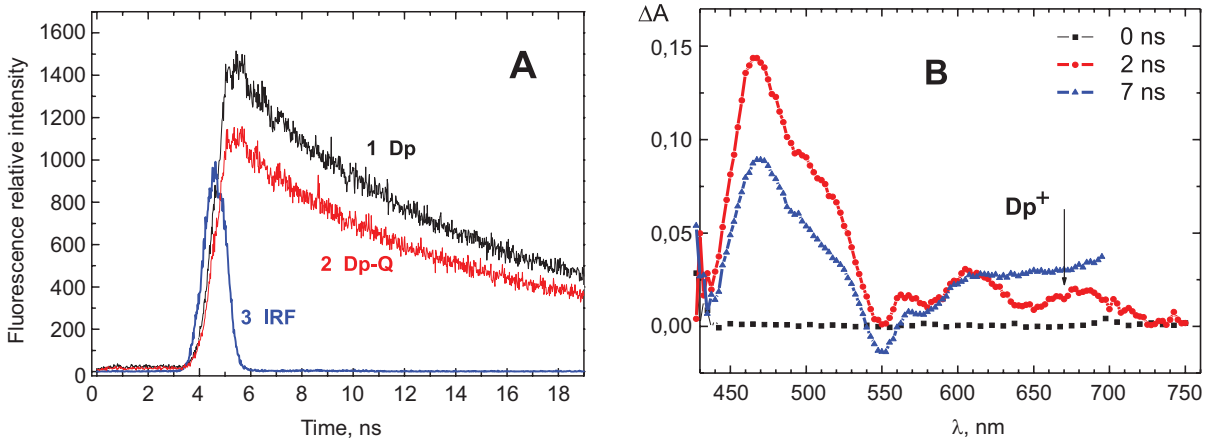

Figure 5. Fluorescence decays (A, λ_{det}=640 nm) detected for **Dp** (1) and the dyad **Dp-Q** (2) and time-resolved absorption spectra (B, λ_{pump}=540 nm) of the dyad **Dp-Q** at delay times 0, 2 and 7 ns in dimethylformamide at 295 K. IRF in (A) corresponds to the experimental response function. Details on pump-probe measurements and home-made experimental setup were described earlier in.[37]

on the solvent polarity. Main details of PET in the systems under study will be discussed later on.

Quantitative Analysis of the Non-radiative Energy Transfer

It was concluded above that the observed experimental findings for the dyad **Trp-Dp** and triad **Trp-Dp-Trp** may be connected with the realization of the non-radiative inductive resonance energy transfer Trp→Dp *via* excited singlet states of D (Trp) and A (Dp) molecules. Correspondingly, using theoretical considerations discussed in[10,11,47-49] one could carry out a quantitative analysis of S-S ET processes for the systems under study.

Currently, because of lack of light emitting diodes in 250-300 nm UV range we have not succeeded to collect time-resolved data for fluorescence decay of Trp alone and in the complexes. But it is possible to estimate S-S ET efficiencies in the dyad *via* the sensibilization of the Dp emission (fluorescence enhancement) using fluorescence excitation and absorption data and approach described in.[52,53] In this case, experimental efficiencies (Φ_{ET}) of Dp fluorescence enhancement caused by S-S ET have been calculated from the direct measurements of the corresponding intensities (I) in fluorescence excitation spectra and optical densities (OD) in absorption spectra of the dyad **Trp-Dp** using the equation

$$\Phi_{ET} = \left[\frac{I_{diad}(\lambda_1) - I_{Dp}(\lambda_1)}{I_{Dp}(\lambda_2)}\right] : \left[\frac{OD_{diad}(\lambda_1) - OD_{Dp}(\lambda_1)}{OD_{Dp}(\lambda_2)}\right]. \quad (1)$$

Here, I_{dyad} corresponds to the Dp fluorescence intensity in the dyad **Trp-Dp**, whereas I_{Dp} is the fluorescence intensity of the individual Dp at the same molar ratio, and λ_1=280 nm, λ_2=398 nm. Based on experimental data it has been estimated that S-S ET efficiencies are as follows: Φ_{ET}=0.75 for the dyad **Trp-Dp** and Φ_{ET}=0.65 for the triad **Trp-Dp-Trp**.

In its turn, based on these data one can estimate the mean donor-acceptor distance R_{DA} using the well-known expression for pair transfer:[47-49]

$$R_{DA}^{exp} = R_0 \cdot \sqrt[6]{\frac{1-\Phi_{ET}}{\Phi_{ET}}}, \quad (2)$$

where R_0 is the critical transfer distance at which the whole deactivation rate constant of S_1 state of the D molecule is equal to the ET rate constant;

$$R_0^6 = \frac{9000 \cdot ln10 \cdot k^2}{128\pi^5 \cdot n^4 N_A} \cdot \varphi_D^0 \int_0^\infty f_D(\nu)\varepsilon_A(\nu)\frac{d\nu}{\nu^4}, \quad (3)$$

$J = \int_0^\infty f_D(\nu)\varepsilon_A(\nu)\frac{d\nu}{\nu^4}$ is spectral overlap integral, $f_D(\nu)$ is the D fluorescence spectrum in wave number scale and normalized to 1 by square, $\varepsilon_A(\nu)$ is the A absorption spectrum measured in $M^{-1}cm^{-1}$, N_A is Avogadro number. The meanings of other parameters are presented in notes for Table 2 collected all calculated parameters for S-S ET in the dyad **Trp-Dp**.

It follows from data presented in Table 2 that for the dyad **Trp-Dp** experimental and theoretical values of ET efficiency are in a reasonable agreement (Φ_{ET}^{exper}=0.75 and Φ_{ET}^{theor}=0.87). It indicates that the Foerster theory of inductive resonance is still applicable to weakly interacting porphyrin and tryptophan π-conjugated systems. Nevertheless, intercenter D-A distances R_{DA}^{exper} (estimated from ET parameters) are relatively high compared to the corresponding values evaluated from the optimized geometries (see Figure 2). This difference may be explained by the overestimation of the orientational factor k^2 values (and thus, R_0^{theor} critical distances) for the dyad **Trp-Dp**. In reality, Trp fluorescence band overlaps with few electronic transitions (forming Soret band in absorption spectra of tetrapyrroles[10,13,15,37,39]) being differently oriented with respect to tetrapyrrole macrocycle. Therefore, the direct calculation of the orientational factor k^2 seems to be very complicated problem. In addition, a high flexibility of a covalent spacer -CH_2-CH_2-COO- followed by a rotation of *D* and *A* molecular subunits (depending on the solvent nature and properties) may also lead to a strong variation of a mutual displacement of interacting dipoles. But in any case, from the obtained results it is evidently clear that folded geometries of A and C types (Figure 2) for the dyad **Trp-Dp** and triad **Trp-Dp-Trp** are thought to be low probable in various liquid solvents.

Table 2. Energy transfer parameters for dyad **Trp-Dp** (toluene, 295 K, refractive index n=1.4968).

φ_D^0	$\varepsilon_A(\nu)$,[b] $M^{-1}\cdot cm^{-1}$	$J(\nu)$, $cm^3\cdot M^{-1}$	k^2 [c]	R_0^{theor}, Å	R_{DA}^{exper},[d] Å	Φ_{ET}^{theor} [e]
0.2[a]	$17.5\cdot10^4$	$12.4\cdot10^{-14}$	0.42 ÷ 0.70	34.0÷38.2	25÷27	0.87

Notes: [a]quantum yield of Trp fluorescence was taken from;[54,55] [b]decimal molar extinction coefficient for Dp in the maximum of Soret band; [c]orientational factors were calculated on the basis of an optimized geometries for the dyad and the inductive-resonant theory[47-49] as

$k^2=[\cos(\mu_D, \mu_A) - 3\cos(\mu_D, r_{DA})\cdot\cos(\mu_A, r_{DA})]^2=0.47\div0.75$, (4)

where (μ_D, μ_A) is the angle between the transition dipole moments of the *D* and *A* subunits, (μ_D, r_{DA}) and (μ_A, r_{DA}) denote the angles between the dipole vectors of *D* and A and the direction vector between *D* and *A*, respectively; [d]R_{DA}^{exper} values were calculated using Eq. (2) and experimentally estimated Φ_{ET} data; [e]theoretical value Φ_{ET}^{theor} was calculated according to[47] as

$\Phi_{ET}^{theor}=(k_{ET})/(k_{ET}+<\tau_D^0>^{-1})$, (5)

where $k_{ET} = \frac{1}{\langle\tau_D^0\rangle}\left(\frac{R_0^{theor}}{R_{DA}}\right)^6$ (6)

and mean value for tryptophan (D) emission decay $<\tau_D^0>$=2.5 ns was taken from.[56]

Quantitative Description of Photoinduced Electron Transfer Processes to Covalently Linked Quinone

With respect to the dyad **Dp-Q** and triad **Trp-Dp-Q**, the corresponding analysis gives the following. Since the absorption spectra for alone Dp and Dp in the dyad **Dp-Q** and triad **Trp-Dp-Q** do not differ practically, we will analyze PET processes in these complexes in terms of the semi-classical Marcus theory[57,58] developed for charge-transfer reactions in the "normal" region. At high temperatures, the semi-classical Marcus theory of endergonic or moderately exergonic non-adiabatic ET occurring within the "normal" region predicts the following expressions for the rate constant k_{PET}:

$$k_{PET}^{S} = \frac{2\pi}{\hbar} \cdot \frac{V_{12}^2}{\left(4\pi\lambda k_B T\right)^{1/2}} \cdot exp\left(-\frac{\Delta G^*}{k_B T}\right) \quad (7)$$

with activation energy $\Delta G^* = \frac{\left(\Delta G^0 + \lambda\right)^2}{4\lambda}$ (8)

Here k_B is Boltzman's constant, T is the temperature, $\hbar = h / 2\pi$, h is Plank's constant, V_{12} is the electronic coupling term between the electronic wave functions of the reactant and product states, $\lambda=\lambda_{in}+\lambda_{ext}$ is the Gibbs reorganisation energy determined by the nuclear λ_{in} and solvent λ_{ext} reorganisation energies, ΔG^0 is the Gibbs free energy of the PET reaction, ΔG^* is the Marcus Gibbs activation energy. For porphyrin macrocycles, the term, λ_{in}, involving vibrational energy changes between the reactant and product states was estimated to be $\lambda_{in} \approx 0.3$ eV.[59,60]

The solvent-dependent term λ_{ext} (λ_{solv}) or for the surrounding medium treated as a dielectric continuum, is expressed as:[57-60]

$$\lambda_{solv} = \frac{e^2}{4\pi\varepsilon_0}\left[\frac{1}{2r_D}+\frac{1}{2r_A}+\frac{1}{r_{DA}}\right]\cdot\left[\frac{1}{\varepsilon_{op}}-\frac{1}{\varepsilon_{st}}\right], \quad (9)$$

where $\varepsilon_{op}=n^2$ is the optical dielectric constant, n is the refraction index and ε_{st} is the static dielectric constant of the solvent (n=1.49693, ε_{st}=2.38 for toluene; n=1.43047, ε_{st}=36.7 for dimethylformamide); r_D=5 Å (for porphyrin macrocycle), r_A=3.3 Å (for quinone);[10,37] r_{DA} is an intercenter Dp-Q distance in the dyad **Dp-Q** and triad **Trp-Dp-Q**. These values have been used for the calculation of PET parameters listed in Table 3.

According to Marcus theory,[57,58] adiabatic PET in a "normal" region becomes possible if the Gibbs free energy of the process $\Delta G^0<0$. With respect to our complexes, Gibbs free energy of PET reaction may be calculated according to[61]

$$\Delta G^0 = E(\mathrm{CT}) - E(\mathrm{S_1^D}) = e(E_D^{OX} - E_A^{RED}) + \Delta G_S - E(\mathrm{S_1^D}). \quad (10)$$

The oxidation potential for porphyrin (E_D^{OX}=0.63 V in dimethylformamide *vs*. SCE) and reduction potential for quinone E_A^{RED}=–0.45 V (in dimethylformamide *vs*. SCE) were taken from literature.[62-64] The correction term ΔG_S accounts for the Coulomb interaction between D and A of the radical ion pair, and was estimated to be $\Delta G_S \leq 0.21$ eV.[37,65] All calculated energetic parameters describing PET processes for the dyad **Dp-Q** are presented in Table 3, thus permitting to quantitatively describe the photoinduced electron transfer events in the systems under study.

Comparative analysis of experimental data being obtained for the dyad **Dp-Q** and triad **Trp-Dp-Q** (see Table 1) shows that the efficiencies of Dp fluorescence quenching due PET do not differ significantly for these two complexes (being a little bit smaller for the triad **Trp-Dp-Q** compared to the dyad **Dp-Q**). It may be explained by the fact that possible steric interactions between covalently linked Trp and Q subunits in the triad do not significantly change the arrangement of Q molecule with respect to a porphyrin macrocycle compared to the dyad **Dp-Q**. Nevertheless, it is seen from Table 1 that transition from non-polar toluene to polar dimethylformamide manifests itself for both complexes in the strengthening of Dp fluorescence quenching as well as an existence of bi-exponential emission decay. According to PET theory,[57-59] the increase of quenching effects upon the solvent polarity increase is typically explained by the stabilization

Table 3. Energies of the donor localized S_1 state, $E(S_1)$, radical ion pair state, E(CT), and PET parameters for the dyad **Dp-Q** in dimethylformamide at ambient temperature (n=1.43047, ε_{st}=36.71).

$E(S_1)$,[a] eV	r_{DA},[b] Å	λ_{solv},[c] eV	λ,[d] eV	E(CT), eV	ΔG^0,[e] eV	ΔG^*,[f] eV	k_{PET},[g] s^{-1}	V_{12},[h] meV
1.99	19	0.77	1.03	1.86	–0.13	0.197	$2.7\cdot10^8$	0.42

Notes: Evaluation of redox potential values for Dp (E_D^{OX}) and Q (E_A^{RED}) as well as D and A radii (r_D and r_A) is described in the text with the corresponding references.

[a]The energy level of Dp locally excited S_1 state was determined on the basis of the corresponding fluorescence and absorption $Q(0,0)$ bands.

[b]Intercenter distances r_{DA} were estimated on the basis of Draiding structural models and molecular modeling taking into account possible steric interactions and are in the range ~ 19 Å.

[c]The solvent-dependent term λ_{solv} was estimated using Eq. (9).

[d]The Gibbs reorganization energy was estimated to be $\lambda=\lambda_{in}+\lambda_{solv}$, ≈ 1.03, where λ_{in} was taken to ~ 0.3 eV.[59,60]

[e]The Gibbs free energy of the PET reaction ΔG^0 was calculated using Eq. (10).

[f]The activation energy ΔG_S was estimated according to Eq. (8).

[g]Calculations of experimental rate constants, k_{PET} for PET with participation of S_1 states of the donor molecule (Dp) were done according to well-known expression:

$$k_{PET} = 1/\tau - 1/\tau^0, \quad (11)$$

where τ^0 and τ are fluorescence decays of unquenched and quenched Dp, correspondingly; taking into account two-exponential decay of Dp emission in the dyad, k_{PET} was found for the shorter component τ_1=3.6 ns of Dp fluorescence decay in the dyad (see Table 1).

[h]The electronic coupling term was calculated on the basis of Eq. (7).

of the energy of the radical ion pair state, E(CT). In its turn, we apt to believe that non-exponential emission decay for Dp in this case may reflect some changes of conformational mobility of the complexes when going to dimethylformamide. Correspondingly, Table 3 collects the estimated PET parameters upon taking into account experimental data for the shorter component of Dp emission decay in the dyad.

Thus, assuming realistic errors for λ and ΔG^0 estimations one may conclude that for the dyad **Dp-Q** in dimethylformamide at 293 K, the Dp fluorescence quenching is appropriately described by Marcus theory of PET in a "normal" region (*i.e.* $-\Delta G^0<\lambda$). In addition, as far as the electronic coupling term V_{12} is smaller than kT=25.7 meV at room temperature, the PET reaction is non-adiabatic in this case. It was mentioned above that steric interactions between covalently linked Trp and Q subunits in the triad **Trp-Dp-Q** do not significantly change the arrangement of Q molecule with respect to a porphyrin macrocycle compared to the dyad **Dp-Q**. Thus, the main peculiarities of PET reaction in dimethylformamide for the triad seem to be the same. It is known also[57-60] that the medium between *D* and *A* strongly influences the rate constant of PET process (through solvent coupling). Correspondingly, when going from polar dimethylformamide to the non-polar toluene, PET efficiency and rate constant decrease significantly and Dp fluorescence quenching is not so pronounced (see Table 1).

Finally, we like to address the question why are PET processes in the dyad **Dp-Q** less pronounced compared to other D-A complexes containing porphyrins and electron acceptors. For instance, in benzene at 293 K, for covalently linked ZnP-Q complexes with smaller D-A distance r_{DA}=13 Å (compared to our case) PET is essentially stronger: $k_{PET}=(6.0–9.5)\cdot10^{10}$ s^{-1} ($\Delta G^0=-0.46\div-0.39$ eV).[66] On the other hand, for the Q-substituted dimer $(ZnOEP)_2$Ph-Q having the same r_{DA} distance and similar Gibbs free energy ΔG^0, in toluene at 293 K the PET rate constant $k_{ET}=2.86\cdot10^{10}$ s^{-1} [11,37] is smaller as compared to the above complex with monomeric porphyrin ZnP-Q. This may be explained by taking into account the competition between the non-radiative S-S energy transfer among monomeric subunits in the dimer $(ZnOEP)_2$Ph and charge separation.[35,37] According to experimental findings and theoretical estimations[11,37] in Zn-porphyrin chemical dimers with intercenter distances of d≈11 – 13 Å, rate constants of the non-radiative S-S energy migration are close to $k_{ET}\approx(3–7)\cdot10^{10}$ s^{-1}. Correspondingly, as far as for the Q-substituted dimer $(ZnOEP)_2$Ph-Q $k_{EM}\leq k_{ET}$, a slower energy transfer process limits the fast PET leading to the relative decrease of the experimental k_{PET} values in the dimers[11,37] with respect to those found for Q-substituted monomers.[66]

Thus, the above comparison and considerations allow us to do some additional conclusions concerning the realization of PET events in the dyad **Dp-Q** and triad **Trp-Dp-Q**. Low PET efficiency in these systems compared to ZnP-Q complexes[66] or Q-substituted dimer $(ZnOEP)_2$Ph-Q[11,37] are explained mainly by larger D-A distances in our case. Moreover, our experimental low k_{PET} values show again that the formation of folded geometries may be excluded for the dyad **Trp-Dp** and triad **Trp-Dp-Q** in dimethylformamide and toluene at ambient temperature. In addition, high flexibility of a covalent spacer -CH_2-CH_2-COO- followed by a rotation of interacting electron *D* and *A* moieties excludes practically the realization of through-bond coupling[59,65] which may strengthen PET efficiency.

Conclusions

From the basic point of view, upon study of properties and possible functionalities of artificial multicomponent organic complexes the basic task seems to be the analysis of spectral-structural correlations as well the mechanisms of interchromophoric interaction depending on the morphology of the given nanostructures.

In this contribution, on the basis steady-state and time-resolved spectral-fluorescent measurements carried out in solutions of various polarity at 295 K for covalently linked dyads and triads (consisting of deuteroporphyrin being attached *via* β-positions to naphthoquinone or to one or two tryptophan residues), the comparative analysis of regularities and mechanisms of the non-radiative deactivation of excited singlet states for tryptophan and porphyrin counterparts has been carried out (including energy transfer and photoinduced electron transfer), and the main parameters determining the efficiency of the processes under consideration have been estimated.

In the case of the dyad **Trp-Dp** experimental and theoretical values of ET efficiency are in a reasonable agreement. It indicates that the Foerster theory of inductive resonance is still applicable to weakly interacting porphyrin and tryptophan π-conjugated systems at intercenter distances $R_{DA}\approx19\div25$ Å. The application of Foerster theory relies on the approximation that the distance R_{DA} between interacting *D* and *A* dipoles is larger than the length $|l|$ of the transition dipoles themselves. The necessary estimations may be derived using well-known expressions[67] for oscillator strength f and transition dipole moment $|\mu|$ of the corresponding low-energy electronic transitions of interacting porphyrin and tryptophan molecules:

$$f = 4.33\times10^{-9}\cdot\varepsilon_{max}(\nu)\Delta\nu_{1/2}, \quad (12)$$

$$f = \left(8\pi^2 m_e \nu|\mu|^2\right)\Big/3he^2, \quad (13)$$

where $\varepsilon_{max}(\nu)$ is the molar decimal extinction coefficient at the maximum of the absorption band and $\Delta\nu_{1/2}$ the corresponding spectral width. Making use of the experimental data known for porphyrins and tryptophan related compounds (having sizes of ~10 Å) we obtain that the effective length of the transition dipoles $|l|\leq1–2.0$ Å for these π-conjugated systems. Consequently, $|l| << R_{DA}$, and it means that in this case the point dipole-dipole approximation is still valid. It should be mentioned in this respect, that the same principal conclusion concerning the application of the weak coupling inductive-resonant model has been done in our early publications for porphyrin chemical dimers[68,69] as well as for self-assembled multiporphyrin complexes.[11,70]

We have shown that for the dyad **Dp-Q** in dimethylformamide at 293 K the Dp fluorescence quenching is due the photoinduced electron transfer Dp→quinone. In the triad **Trp-Dp-Q**, steric interactions between covalently linked Trp and Q subunits do not significantly change the arrangement of Q residues with respect to a porphyrin macrocycle compared to the dyad **Dp-Q**. In these complexes, the Gibbs free energy of PET is ΔG^0=–0.13 eV<0, while the Gibbs reorganisation energy is estimated to be λ=1.03 eV, that is $-\Delta G^0<\lambda$. Correspondingly, the photoinduced electron transfer process in the given dyad may be appropriately described by the semi-classical Marcus theory as an endergonic or moderately exergonic PET occurring within the "normal" region. Moreover, as far as the electronic coupling term V_{12}=0.42 meV is smaller than kT=25.7 meV at room temperature, the PET reaction is non-adiabatic in this case. It is known also,[50] that PET reaction is non-adiabatic by Landau-Zener criteria if it satisfies the following relationship

$$4\pi^2 V^2/h\omega(2\lambda k_B T)^{1/2} < 1, \quad (14)$$

where ω~100 cm^{-1} for typical low-frequency solvent motions at 300 K. It follows from above presented data that for the dyad **Dp-Q** and the triad **Trp-Dp-Q** this criterion is operative in both solvents. Thus, assuming realistic errors for λ and ΔG^0 estimations one may conclude that at ambient temperature the porphyrin S_1-state quenching is due to the non-adiabatic PET. Such conclusions with respect to PET mechanisms have been done by us earlier for multiporphyrin complexes containing covalently linked quinone derivatives.[11,37] It should be mentioned also that high flexibility of a covalent spacer -CH_2-CH_2-COO- followed by a rotation of interacting electron *D* and *A* moieties excludes practically the realization of through-bond coupling[59,65] which may strengthen PET efficiency.

Finally, taken together, the quantitative experimental and theoretical analysis of both energy and photoinduced electron transfer processes for the systems under study leads to the conclusion that the formation of folded geometries (types B, C, see Figure 2) is hardly realized for the dyads **Trp-Dp, Dp-Q** and triads **Trp-Dp-Trp, Trp-Dp-Q** in liquid solvents at ambient temperature.

Acknowledgements. Financial support from the program BSPSR "Convergence–2020 3.03" and BRFBR Grant №Ф18Р-314.

References

1. Tietz C., Jelezko F., Gerken U., Schuler S., Schubert A., Rogl H., Wrachtrup J. *Biophys. J.* **2001**, *81*, 556–562.
2. Cheng Y.C., Fleming G.R. *Annu. Rev. Phys. Chem*. **2009**, *60*, 241–262.
3. Gall A., Sogalia E., Gulbinas V., Ilioaia O., Robert B., Valkunas L. *Biochim. Biophys. Acta* **2010**, *1797*(8), 1465–1469.
4. Freiberg A., Trinkunas G. In: *Unraveling the Hidden Nature of Antenna Excitations* (Laisk A., Nedbal L., Govindjee, Eds.) Amsterdam: Springer Science+Media B.V., **2009**. p. 55–82.
5. Unterkofler S., Pflock T., Southall J., Cogdell R.J., Koehler J. *ChemPhysChem* **2011**, *12*, 711–716.
6. Snellenburg J.J., Johnson M.P., Rubanc A.V., van Grondelle R., Stokkum I.H.M. *BBA Bioenergetics* **2017**, *1858*(10), 854–864.
7. Wibmer L., Lourenco L.M.O., Roth A., Katsukis G., Neves M.G.P., Cavaleiro J.A.S., Tomé J.P.C., Torres T., Guldi D.M. *Nanoscale* **2015**, *7*, 5674–5682.
8. Lee S.-H., Blake I.M., Larsen A.G., McDonald J.A., Ohkubo K., Fukuzumi S., Reimers J.R., Crossley M.J. *Chem. Sci.* **2016**, *7*, 6534–6550.
9. Kundu S., Patra A. *Chem. Rev.* **2017**, *117*, 712–757.
10. *Multiporphyrin Arrays: Fundamentals and Applications* (Kim D., Ed.) Singapore: Pan Stanford Publishing Pte. Ltd., **2012**. 775 p.
11. Zenkevich E.I., von Borczyskowski C. Biophysical and Physicochemical Studies of Tetrapyrroles. In: *Handbook of Porphyrin Science with Application to Chemistry, Physics, Materials Science, Engineering, Biology and Medicine. Vol. 22 – Biophysical and Physicochemical Studies of Tetrapyrroles* (Kadish K., Smith K.M., Guilard R., Eds.) Singapore: World Scientific Publishing Co. Pte. Ltd., **2012**. p. 67–168.
12. Fukuzumi S., Lee Y.-M., Nam W. *ChemPhotoChem* **2018**, *2*, 121–135.
13. Mora S.J., Odella E., Moore G.F., Gust D., Moore T.A., Moore A.L. *Acc. Chem. Res.* **2018**, *51*, 445−453.
14. Hood D., Sahin T., Parkes-Loach Pamela S., Jiao J., Harris Michelle A., Dilbeck P., Niedzwiedzki D.M., Kirmaier C., Loach P.A., Bocian D.F., Lindsey J.S., Holten D. *ChemPhotoChem* **2018**, *2*, 300–313.
15. Otsuki J. *J. Mater. Chem. A* **2018**, *6*, 6710–6753.
16. Nicolini C. Nanoscale Materials. In: *Nanotechnology and Nanobiosciences*. Singapore: Pan Stanford Publishing Pte. Ltd., **2010**. 367 p.
17. Self-Assembled Organic-Inorganic Nanostructures: Optics and Dynamics (Zenkevich E., von Borczyskowski C., Eds.) Singapore: Pan Stanford Publishing Pte. Ltd., **2016**. 394 p.
18. *Nano- and Biocomposites.* (Lau A.K-t., Hussain F., Lafdi K., Eds.) CRC Press, **2017**. 408 p.
19. Shikinaka K. *Functionalization of Molecular Architectures: Advances and Applications on Low-Dimensional Compounds.* Singapore: Pan Stanford Publishing Pte. Ltd., **2018**. 350 p.
20. Ahmed S., Kanchi S. *Handbook of Bionanocomposites*. Singapore: Pan Stanford Publishing Pte. Ltd., **2018**. 318 p.
21. *Handbook of Porphyrin Science with Application to Chemistry, Physics, Materials Science, Engineering, Biology and Medicine. Volumes 1 "Supramolecular Chemistry", 4 "Phototherapy, Radioimunotherapy and Imaging", 10 "Catalysis and Bio-Inspired Systems"* (Kadish K., Smith K.M., Guilard R., Eds.) Singapore: World Scientific Publishing Co. Pte. Ltd., **2010**.
22. *Handbook of Carbon Nano Materials. Vol. 1 – Synthesis and Supramolecular Systems, Vol. 2 – Electron Transfer and Applications* (D'Souza F., Kadish K.M., Eds.) Singapore: World Scientific Publishing Co. Pte. Ltd., **2011**.
23. Murchison H.A., Alden R.G., Allen J.P., Peloquin J.M., Taguchi A.K.W., Woodbury N.W., Williams J.C. *Biochemistry* **1993**, *32*, 3498–3505.
24. Heller B.A., Holten D., Kirmaier C. *Biochemistry* **1995**, *34*, 5294–5302.
25. Chan C.K., Cher L.X.-Q., Di Magno T.J., Hanson D.K., Nance S.L., Schiffer M., Norris J.K., Fleming G.R. *Chem. Phys. Lett.* **1991**, *176*, 366–372.
26. Alden R.G., Parson W.W., Chu Z.T., Warshel A. *J. Phys. Chem.* **1996**, *100*, 16761–16770.
27. Michel H., Deisenhofer J. *Biochemistry* **1988**, *27*, 1–7.
28. Allen J.P., Williams J.C. *FEBS Lett.* **1998**, *438*, 5–9.
29. Shuvalov V.A. *Transformation of Solar Energy in the Primary Act of Charge Separation in the Reaction Centers of Photosynthesis.* Moscow: Nauka, **2000**. 50 p. (in Russ.)

[Шувалов В.А. *Преобразование солнечной энергии в первичном акте разделения зарядов в реакционных центрах фотосинтеза.* М.: Наука, **2000**. 50 с.].
30. Rodriguez J., Kirmaier C., Johnson M.R., Friesner R.A., Holten D., Sessler J.L. *J. Am. Chem. Soc.* **1991**, *113*, 1652–1659.
31. Borovkov V.V., Gribkov A.A., Kozyrev A.N., Brandis A.S., Ishida A., Sakata Y. *Bull. Chem. Soc. Jpn*. **1992**, *65*, 1533–1537.
32. Gribkova S.E., Evstigneeva R.P., Luzgina V.N. *Russ. Chem. Rev.* **1993**, *62*, 963–979.
33. Okomoto K., Fukuzumi S. *J. Phys. Chem*. *B* **2005**, *109*, 7713.
34. Häbele T., Hirsch J., Pöllinger F., Heitele H., Michel-Beyerle M.E., Anders C., Döhling A., Krieger C., Rückemann A., Staab H.A. *J. Phys. Chem.* **1996**, *100*, 18269–18274.
35. Rempel U., Meyer S., von Maltzan B., von Borczyskowski C. *J. Lumin.* **1998**, *78*, 97.
36. Wiehe A., Senge M.O., Schafer A., Speck M., Tannert S., Kurreck H., Roeder B. *Tetrahedron* **2001**, *57*, 10089–10110.
37. Zenkevich E.I., von Borczyskowski C., Shulga A.M., Bachilo S.M., Rempel U., Willert A. *Chem. Phys.* **2002**, *275*, 185–209.
38. Gurinovich G.P., Sevchenko A.N., Solovyov K.N. *Spectroscopy of Chlorophyll and Related Compounds*. Minsk, USSR: Science and Engineering Publishing, **1968**. 517 p. (Engl. transl. by U.S. Atomic Energy Commission, Division of Technical Information, Springfield, VA 22151, 1971, 506 p., Pub ID: 101-653-364).
39. Falk J.E. *Porphyrins and Metalloporphyrins*. Amsterdam–London–New York: Elsevier Pub. Co., **1964**. 266 p.
40. Borovkov V.V., Fillipovich E.I., Evstigneeva R.P. *Chem. Heterocycl. Compd*. **1988**, *24*, 494.
41. Larkina E.A., Luzgina V.N., Evstigneeva R.P. *Russ. J. Bioorg. Chem.* **2002**, *28*, 322–325.
42. Larkina E.A., Balashova T.A., Luzgina V.N., Konovalova N.V., Evstigneeva R.P. *Mendeleev Commun*. **2005**, 234–236.
43. Zenkevich E.I., Sagun E.I., Knyukshto V.N., Stasheuski A.S., Galievsky V.A., Stupak A.P., Blaudeck T., von Borczyskowski C. *J. Phys. Chem. C* **2011**, *115*, 21535–21545.
44. Parker C.A. *Photoluminescence of Solutions*. Amsterdam–London–New York: Elsevier Pub. Co., **1968**. 544 p.
45. Egorova G.D., Knyukshto V.N., Solov'ev K.N., Tsvirko M.P. *Opt. Spektrosk.* **1980**, *48*, 1101.
46. *CRC Handbook of Chemistry and Physics* (Lide D.R., Ed.) CRC Press LLC, 82nd Edition, Corporate Blvd. N.W., Boca Raton, FL 3343, **2002**.
47. Foerster T. *Modern Quantum Chemistry* (Sinanoglu O., Ed.) New York: Academic Press, **1965**.
48. Agranovich V.M., Galanin M.D. *Electronic Excitation Energy Transfer in Condensed Matter.* Amsterdam, New York: North-Holland Pub. Co., **1982**. 371 p.
49. Ermolaev V.L., Bodunov E.N., Sveshnikova E.B., Shakhverdov T.A. *Non-Radiative Electronic Excitation Energy Transfer*. Leningrad: Nauka, **1977**. 311 p.
50. Johnson D.J., Niemczyk M.P., Minsek D.W., Wiererrechy G.P., Svec W.A., Gaines III G.L., Wasielewski M.R. *J. Am. Chem. Soc*. **1993**, *115*, 5692–5701.
51. Furhop J.-H., Mauzerall D. *J. Am. Chem. Soc*. **1969**, *91*, 4174–4181.
52. Zenkevich E., Cichos F., Shulga A., Petrov E., Blaudeck T., von Borczyskowski C. *J. Phys. Chem. B.* **2005**, *109*, 8679–8692.
53. Zenkevich E.I., Gaponenko S.V., Sagun E.I., von Borczyskowski C. *Reviews in Nanoscience and Nanotechnology* **2013**, *2*(3), 184–207.
54. Kochubeyev G.A., Frolov A.A., Zenkevich E.I., Gurinovich G.P. *Dokl. Akad. Nauk BSSR* **1988**, *32*, 175–182 (in Russ.).
55. McGimpsey W.G., Gorner H. *Photochem. Photobiol.* **1996**, *64*, 501–509.
56. Albani J.R. *J. Fluoresc.* **2013**, *24*, 105–117.
57. Marcus R.A. *Rev. Modern Phys*. **1993**, *65*, 599–610.
58. Sutin N. In: *Electron Transfer in Inorganic, Organic, and Biological Systems* (Bolton J.M., Mataga N., McLendon J., Eds.) Washington: Am. Chem. Soc., CSC Symposium Series, **1991**. p. 25–47.
59. Wasielewski M.R., Gaines III G.L., O'Neil M.P., Svec W.A., Niemczyk M.P., Prodi L., Gosztola D. In: *Dynamics and Mechanisms of Photoinduced Transfer and Related Phenomena* (Mataga N., Okada T., Masuhara H., Eds.). Amsterdam: Elsevier Science Publishers, **1992**. p. 87–103.
60. Heitele H., Michel-Beyerle M.E. *J. Am. Chem. Soc*. **1985**, *107*, 8286.
61. Rehm D., Weller A. *Isr. J. Chem*. **1970**, *8*, 259.
62. Sagun E.I., Zenkevich E.I., Knyukshto V.N., Shulga A.M., Ivashin N.V. *Opt. Specktrosk.* **2010**, *108*, 590–607. (in Russ.).
63. Murrov S.L., Carmichael I., Hug G.L. In: *Handbook of Photochemistry.* New-York-Basel-Hong Kong: Marcel Deccer, Inc. **1993**. p. 269–278.
64. Mayranovskiy V.G. Electrochemistry of Porphyrins. In: *Porphyrins: Spectroscopy, Electrochemistry, Application* (Yenikopolyan N.S., Ed.), Moscow: Nauka, **1987**. p. 127–181 (in Russ.) [Майрановский В.Г. Электрохимия порфиринов. В кн.: *Порфирины: спектроскопия, электрохимия, применение* (Ениколопян Н.С., ред.), М.: Наука, **1987**. с. 127–181].
65. Sagun E.I., Zenkevich E.I., Knyukshto V.N., Shulga A.M., Tikhomirov S.A. *Proc. SPIE*, Vol. 6727, ICONO 2007: Nonlinear Laser Spectroscopy and High-Precision Measurements; and Fundamentals of Laser Chemistry and Biophotonics (Tikhomirov S.A., Udem T., Yudin V., *et.al.*, Eds.) **2007**. p. 67272U.
66. Asahi T., Ohkohchi M., Matsusaka R., Mataga N., Zang R.P., Osuka A., Maruyama K. *J. Am. Chem. Soc*. **1993**, *115*, 5665.
67. Atkins P., de Paula J. *Atkin's Physical Chemistry*. Oxford: Oxford University Press, 7th Ed., **2002**. 577 p.
68. Gurinovich G.P., Zenkevich E.I., Sagun E.I., Shulga A.M. *Opt. Specktrosk.* **1984**, *56*, 1037–1043 (in Russ.).
69. Zenkevich E.I., Shulga A.M., Sagun E.I., Gurinovich G.P., Chernook A.V. *Teubner-Texte zur Physik*, Leipzig: BSB B.G. Teubner Verlagsgesselschaft, **1985**, Band 4, 297–300.
70. Chernook A.V., Shulga A.M., Zenkevich E.I., Rempel U., von Borczyskowski C. *Ber. Bunsenges. Phys. Chem.* **1996**, *100*, 114–118.

Received 10.01.2019
Accepted 29.01.2019